Title
Back Cover: Highly Selective Condensation of Biomass-Derived Methyl Ketones as a Source of Aviation Fuel (ChemSusChem 10/2015)

Journal
ChemSusChem, 8(10)

ISSN
1864-5631

Authors
Sacia, Eric R
Balakrishnan, Madhesan
Deaner, Matthew H
et al.

Publication Date
2015-05-22

DOI
10.1002/cssc.201500556

Peer reviewed

ChemPubSoc Europe

DOI: 10.1002/cssc.201500002

CHEMSUSCHEM Full Papers

Highly Selective Condensation of Biomass-Derived Methyl Ketones as a Source of Aviation Fuel

Eric R. Sacia,[a] Madhesan Balakrishnan,[a] Matthew H. Deaner,[a] Konstantinos A. Goulas,[a, b] F. Dean Toste,[b] and Alexis T. Bell*[a]

Aviation fuel (i.e., jet fuel) requires a mixture of C_9–C_{16} hydrocarbons having both a high energy density and a low freezing point. While jet fuel is currently produced from petroleum, increasing concern with the release of CO_2 into the atmosphere from the combustion of petroleum-based fuels has led to policy changes mandating the inclusion of biomass-based fuels into the fuel pool. Here we report a novel way to produce a mixture of branched cyclohexane derivatives in very high yield (>94%) that match or exceed many required properties of jet fuel. As starting materials, we use a mixture of *n*-alkyl methyl ketones and their derivatives obtained from biomass. These synthons are condensed into trimers via base-catalyzed aldol condensation and Michael addition. Hydrodeoxygenation of these products yields mixtures of C_{12}–C_{21} branched, cyclic alkanes. Using models for predicting the carbon number distribution obtained from a mixture of *n*-alkyl methyl ketones and for predicting the boiling point distribution of the final mixture of cyclic alkanes, we show that it is possible to define the mixture of synthons that will closely reproduce the distillation curve of traditional jet fuel.

Introduction

Aviation fuels must meet a number of stringent specifications, the most significant of which are high energy-density to maximize aircraft range and low freezing-point to avoid formation of crystalline wax particles during high-altitude flight. These requirements are readily met by branched and cyclic hydrocarbons, and, consequently, these types of fuels are not likely to be displaced for air transportation. On the other hand, significant growth in the consumption of aviation fuel[1] and concerns about anthropogenic CO_2 emissions have led to increasing policy mandates to create biomass-derived hydrocarbons for the aviation industry.[1,2] For this reason, the International Air Transport Association aspires to reach 6% blends of biofuels in standard jet fuel by 2020, a target which would have required 5.0 billion liters of biofuel for the United States alone in 2011.[2a] Biomass-based aviation fuels could also qualify in the US for the Renewable Fuels Standard and in the EU for the Renewable Energy Directive.[2b]

Several technologies have been evaluated for the production of biomass-derived jet fuel.[3] The processes that are closest to commercialization are hydroprocessed esters and fatty acids (HEFA), Fisher–Tropsch jet fuel (FTJ), and pyrolysis jet fuel (PJ).[1,3] However, each of the processes used to produce these fuels has its drawbacks. The use of vegetable oils to produce HEFA has led to increases in food costs in some parts of the world and is difficult to produce sustainably with high fuel yields per acre.[4] Moreover, the linear alkanes formed by decarboxylation and hydrogenation of vegetable oils must undergo hydrocracking and isomerization to reduce their molecular weight and introduce branching.[1,5] FTJ and PJ technologies can use non-edible lignocellulosic feedstocks but suffer from low overall process yields and the high energy demand to carry out biomass gasification or pyrolysis.[3] It should also be noted that pyrolysis oil must be hydrodeoxygenated to comply with regulations and to improve fuel stability.

The preceding discussion suggests that alternative approaches should be considered for converting biomass to jet fuel. For example, branched alkanes in the required C_9–C_{16} range can be produced in high selectivity and in the absence of solvent by furan condensation[6] followed by hydrodeoxygenation.[7] Alternatively, butenes, derived from γ-valerolactone, can be oligomerized to produce C_8, C_{12}, and C_{16} alkenes, which can then be hydrogenated to yield mostly branched alkanes.[8] A drawback of this approach is that, at high butene conversions, the selectivity to jet fuel hydrocarbons (C_8–C_{16}) cannot be maintained due to formation of higher oligomers (C_{16+}).[8] Yet another alternative is the dimerization of angelica lactone, derived from levulinic acid (LA). This strategy produces C_7–C_{10} intermediates, which after hydrodeoxygenation, yield highly branched alkanes.[9] However, these products are too volatile to be used in significant fractions as components of jet fuel. Since conventional jet fuel contains approximately 20% cyclic alkanes, the production of such hydrocarbons from biomass is

[a] Dr. E. R. Sacia,[+] Dr. M. Balakrishnan,[+] M. H. Deaner, K. A. Goulas, Prof. A. T. Bell
Department of Chemical and Biomolecular Engineering
University of California, Berkeley
107 Gilman Hall, Berkeley, CA 94720 (USA)
E-mail: bell@cchem.berkeley.edu

[b] K. A. Goulas, Prof. F. D. Toste
Department of Chemistry
University of California, Berkeley
107 Gilman Hall, Berkeley, CA 94720 (USA)

[+] These authors contributed equally to this work.

Supporting Information for this article is available on the WWW under http://dx.doi.org/10.1002/cssc.201500002.

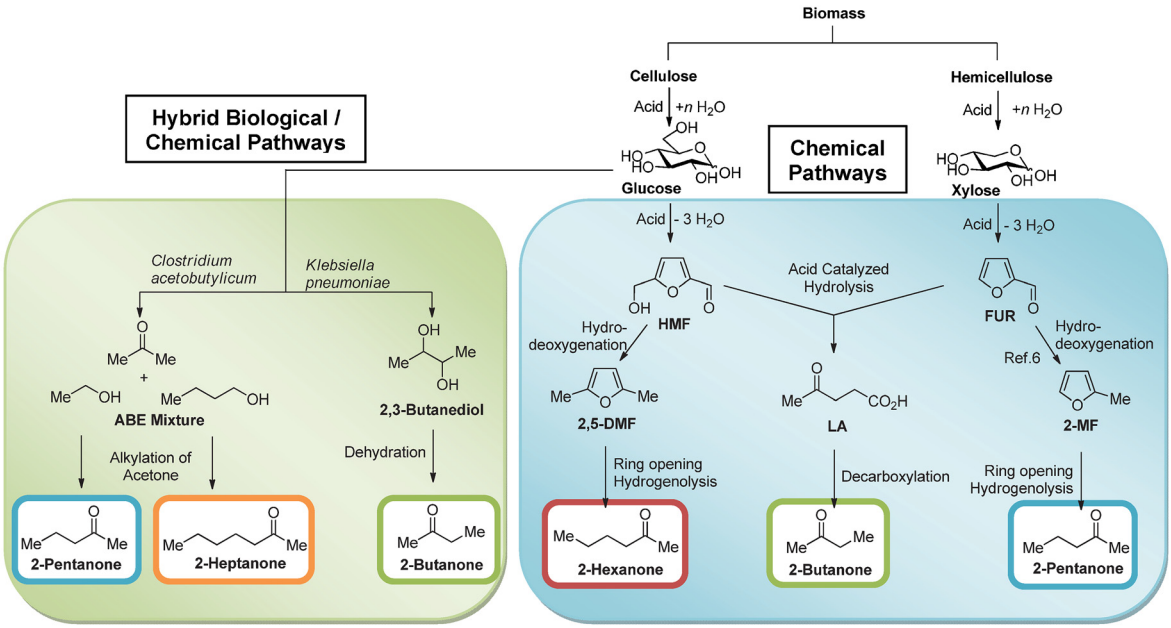

Figure 1. Overview of production of methyl ketones from biomass.

especially attractive.[10] Recent reports have shown that such cyclic alkanes can be produced from biomass using pinenes[11] and cyclopentanone[12] and that they do possess exceptional fuel properties.

Here we report a novel approach for producing a mixture of cyclic alkanes that replicates the boiling point distribution of jet fuel, exhibits very high energy density, and has excellent cold flow properties. Our strategy involves the catalytic self- and cross-condensation of biomass-derived alkyl methyl ketones and subsequent hydrodeoxygenation of the resulting condensates to create a biomass-derived platform technology for fuels and specialty chemicals. The starting ketones, including 2-butanone, 2-pentanone, 2-hexanone, and 2-heptanone, can be sourced from biomass-derived C_5 and C_6 sugars via the processes shown in Figure 1. Both lignocellulosic and traditional biofuels crops, such as corn and sugarcane, can be used to produce useful sugars for this process. Fermentation of sugars to 2,3-butanediol has been known for over 100 years, and present microbial strains can produce this product from glucose in titers above 150 g L^{-1}.[13] Using hybrid biological-chemical pathways, 2-butanone can be formed in high selectivity (>90%) in the aqueous phase by acid-catalyzed dehydration of 2,3-butanediol,[14] after which it can easily be separated by extraction or distillation. 2-butanone can also be produced from sugar-derived levulinic acid via chemical[15] and hybrid chemical/biological pathways.[16]

Additionally, 2-hexanone can be formed in high selectivity (98%) by hydrogenation of 2,5-dimethylfuran (DMF),[7b] a platform molecule formed in high yield from 5-hydroxymethylfurfural (HMF).[17] 2-pentanone can also be formed in the same selectivity by hydrogenation of 2-methylfuran (MF), a product of xylose-derived furfural (FUR) hydrogenation.[7b] Formation of 2-pentanone and 2-heptanone has also been demonstrated by the mono-alkylation of products obtained from ABE fermentation (acetone, 1-butanol, and ethanol) (Figure 1).[18] While the maximum reported selectivity of each of the above-mentioned methyl ketone-producing steps is typically in excess of 90%, the number of processing steps to provide methyl ketones from biomass should be minimized to limit the number of separations and diminished process yields associated with additional process steps.

While aldol condensation of biomass-derived aldehydes, such as HMF or FUR, with acetone is well established,[19] the condensation of biomass-derived alkyl methyl ketones has received much less attention. An example of this type of reaction is the base-catalyzed condensation of acetone to form a cyclic trimer condensate (isophorone), as well as dimer condensates (mesityl oxide), larger oligomers, and aromatic products (mesitylene).[20] Formation of cyclic trimer condensates, like isophorone, is especially interesting due to the high energy density and low freezing points of cyclic alkanes. However, production of cyclic trimer condensates from larger *n*-alkyl methyl ketones has not been well studied due to the increased steric hindrance provided by larger alkyl substitution. For example, condensation of 2-butanone was previously found to yield cyclic trimer condensates in yields of only 24%.[21] Hence, the main objective of our work was to identify catalysts and reaction conditions that would promote a platform jet fuel production pathway through the selective condensation of methyl ketones to cyclic trimer condensates (**3**) or aromatic products (**5**) while minimizing formation of dimer condensates (**2**), acylic trimer condensates (**4**), and larger oligomers, as shown in Scheme 1.

Results and Discussion

Catalyst selection

Catalysts for condensation of methyl ketones were screened using 2-hexanone as the reactant (Table 1). Because of the superior quality of cyclic fuel products, we sought catalysts

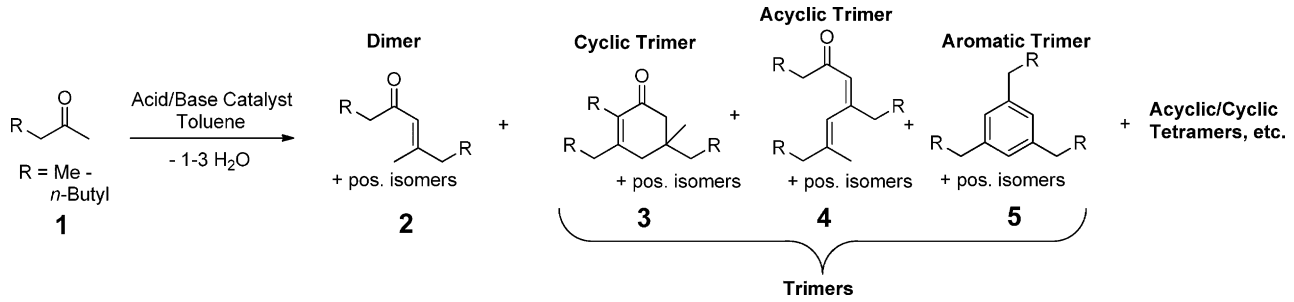

Scheme 1. Typical products of methyl ketone condensation by heterogeneous catalysis.

Table 1. Catalyst screening for the condensation of 2-hexanone.[a]

Entry	Catalyst	*T* [°C]	*t* [h]	Conv. of **1** [%]	Dimers (**2**) [%]	Trimers [%] cyclic (**3**)	Trimers [%] aromatic (**5**)	Total prod. [%]
1	K_3PO_4	180	12	2	0	0	0	0
2[b]	NaOH (1 wt%)	180	1	32	19	9	1	29
3[b]	KOH (1 wt%)	180	1	55	7	43	1	51
4	KF/Al_2O_3 (5 mol%)	150	3	35	21	13	0	34
5	MgO	150	3	98	3	69	0	72
6	Mg-Al-O	150	3	100	0	93	0	93
7	Mg-Al-O (100 mg)	150	3	100	0	92	0	92
8	Mg-Al-O (50 mg)	150	3	96	3	86	0	89
9	Mg-Zr-O	150	3	77	37	32	0	69
10	La_2O_3	150	3	83	10	63	4	77
11	HAP	150	3	76	46	15	7	68
12	TiO_2	150	3	99	0	76	16	92
13	ZrO_2	150	3	89	9	42	19	70
14	Ti-Zr-O	150	3	96	1	54	30	85
15	$SrTiO_3$	150	3	67	55	1	1	57
16	SiO_2-Al_2O_3	150	3	80	22	23	8	54
17	Nb_2O_5	180	3	76	4	5	53	62
18	$NbOPO_4$	180	3	82	19	3	43	65

[a] Reagents and conditions: 2-hexanone (2 mmol), toluene (3 mL), 200 mg of catalyst unless otherwise stated. [b] Run in solvent-free conditions with 1 g of 2-hexanone; Mg-Al-O = Calcined Hydrotalcite (Mg/Al = 3); HAP = Hydroxyapatite.

which could selectively produce cyclic (**3**) and aromatic (**5**) trimer condensates. The results of catalyst screening are given in Table 1.

While K_3PO_4 is an effective aldol condensation catalyst for other systems,[18] entry 1 of Table 1 shows that very little of the starting material is consumed even for long reaction times and high temperatures. Strong bases such as solid NaOH and KOH have been used previously for acetone trimerization.[22] We observed that the reaction of 2-hexanone proceeded readily in the absence of a solvent (entries 2 and 3), but the catalyst underwent dissolution in the by-product, water, making catalyst recovery impractical. The higher reactivity of KOH compared to NaOH is attributed to the relative reactivity of the corresponding enolates (entries 2 and 3).[23]

Traditional heterogeneous bases were also screened for condensation of 2-hexanone. While KF/Al_2O_3 (Table 1, entry 4) showed some activity, low selectivity to the desired condensates and the limited water tolerance of the catalyst make it a poor choice. Alkaline earth metal oxides such as MgO and mixed metal oxides are among the most studied catalysts for self-condensation of acetone due to their significant activity towards isophorone production.[20a,b] While MgO (entry 5) was highly active, its high basicity produced higher oligomers and strongly adsorbed species, as evidenced by significant darkening of the catalyst after reaction.

A routine technique for improving the activity and selectivity of MgO is to add a dopant, such as Al or Zr.[24] Incorporation of Al (a stronger Lewis acid than Mg) into the MgO framework has been observed to increase the number of acid–base pairs with appropriate strength to achieve high turnover frequencies for aldol condensation.[24] Moreover, the Lewis acidic Al site can help to stabilize negatively charged adsorbed intermediates.[24] We observed that, in contrast to MgO, the use of hydrotalcite-derived Mg-Al-O (Mg/Al = 3) resulted in complete reactant consumption, even for low catalyst loadings. More importantly, this catalyst exhibited exceptional selectivity to cyclic trimer condensates under all reaction conditions explored (entries 6–8). Other dopants such as Zr were less effective in providing high yields of trimers (entry 9). La_2O_3, another highly basic material, exhibited high activity (entry 10) despite its low surface area (Supporting Information); however, similar to MgO, its selectivity to the targeted trimer products was lower than that of Mg-Al-O.

An increased selectivity to aromatic products was observed for catalysts containing acid–base pairs with increased acidity, for example TiO_2, ZrO_2, and their mixed oxides. Highly acidic materials, such as amorphous aluminosilicate materials and niobium(V) oxides and phosphates produced significant fractions of aromatic products (**5**). Reduced overall product yield in these reactions (entries 16–18) is attributed to the occurrence of further oligomerization, cracking, and other unknown reaction pathways on the solid acid which may be promoted more significantly by higher Hammett acidity. Because of its high relative activity and high selectivity for the formation of

cyclic trimer condensates, we chose hydrotalcite-derived Mg-Al-O (Mg/Al = 3) for further investigation.

Factors influencing catalytic activity and selectivity

Having selected Mg-Al-O as an exceptional catalyst for the self-condensation of 2-hexanone, we set out to elucidate the functionality of Mg-Al-O responsible for its uniquely high activity and selectivity for production of cyclic trimer condensates. To generate the catalytically active, cubic Mg-Al-O, the brucite-like structure of hydrotalcite materials must first be calcined at high temperature. This calcination procedure also increases the surface area and simultaneously generates Lewis basic sites.[25] Both the basic and acidic sites of Mg-Al-O have been characterized previously in the literature.[26]

To identify the roles of acidic and basic sites in the self-condensation of 2-hexanone, reactions were performed in the presence of various amounts of titrants such as acetic acid or pyridine (see Table 2). Acetic acid bound to the basic sites of Mg-Al-O completely deactivated the catalyst at ratios above 1 mmol g^{-1} catalyst. Since no significant change occurred in either activity or selectivity upon pyridine addition, regardless of concentration, we conclude that the acidic sites of Mg-Al-O do not significantly participate in the mechanism of cyclic trimer formation, consistent with previous reports for acetone on MgO.[20a,b]

We also sought to determine the stability of the catalyst under reaction conditions and in the presence of water, which is produced during reaction. Previous studies have shown that the exposure of water to Mg-Al-O causes a loss of surface area, regeneration of Brønsted basicity, and reformation of the brucite-like structure of hydrotalcite.[25d] Because water is produced as a byproduct of the condensation reactions studied in this work, we were interested in defining the effects of water on the activity and selectivity of Mg-Al-O for 2-hexanone condensation. To this end, Mg-Al-O was subjected to six successive catalytic cycles in the Q-tube reactors to assess its stability. This number corresponds to approximately 520 turnovers per site using the number of basic sites as measured by CO_2 temperature-programmed desorption (Supporting Information). The conversion of 2-hexanone decreased from 99% in the first two cycles to 70% by the sixth cycle; however, recalcination of the catalyst was shown to completely regenerate the original catalyst activity, as is consistent with previous reports of aldol condensations with Mg-Al-O[27] (see Supporting Information). X-ray diffraction (XRD) patterns of catalyst taken after three cycles showed little difference compared to that of the calcined hydrotalcite (Mg-Al-O) and did not display the characteristic peaks of the brucite-like hydrotalcite precursors, as shown in Figure 2.

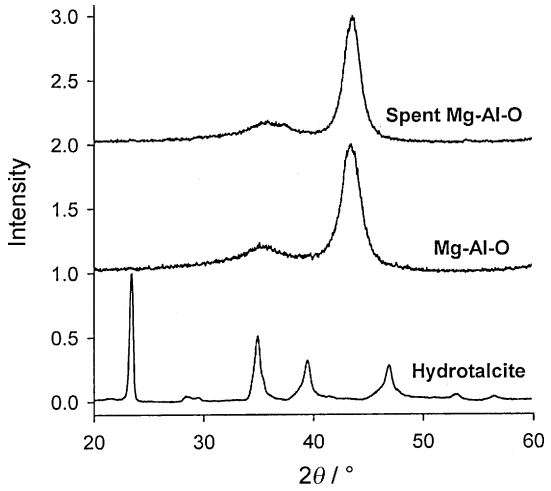

Figure 2. XRD pattern of as-received hydrotalcite, Mg-Al-O, and spent Mg-Al-O (Reaction Conditions: 2-hexanone (2 mmol), toluene (3 mL), 170 °C, 2 h, 100 mg of Mg-Al-O).

The water tolerance of Mg-Al-O at higher water concentrations was also tested by introducing increasing amounts of water into the initial reaction solution. The data in Figure 3 clearly demonstrate the ability of water to inhibit the activity of the catalyst for condensation of methyl ketones. The loss in activity can be attributed to a loss in surface area of Mg-Al-O, due to changes in the catalyst structure, and to inhibition of reversible steps in the condensation mechanism, leading to a shift in equilibrium. In order to mitigate the effects of water during bulk synthesis, we carried out reactions in a Dean–Stark apparatus to continuously remove water from the reaction mixture. This technique proved very effective at maintaining the catalyst activity during large-scale syntheses discussed in the Supporting Information, even at milder temperatures.

Table 2. Effect of acid/base titration on Mg-Al-O activity during the condensation of 2-hexanone.[a]

Entry	Acetic acid [μmol]	Pyridine [μmol]	Mg-Al-O [mg]	Conv. of **1** [%]	Dimers (**2**) [%]	Trimers [%] cyclic (**3**)	acyclic (**4**)	Higher oligomers [%]
1	–	–	100	99	1	95	2	1
2	10	–	100	98	1	93	2	2
3	50	–	100	62	23	38	1	0
4	100	–	100	2	1	0	0	0
5	200	–	100	0	0	0	0	0
6	–	10	100	99	1	95	2	1
7	–	50	100	98	1	95	2	1
8	–	100	100	99	0	95	2	2
9	–	200	100	99	1	95	2	2
10	200	–	–	0	0	0	0	0
11	–	200	–	0	0	0	0	0

[a] Reagents and conditions: 2-hexanone (2 mmol), toluene (3 mL), 170 °C, 2 h, 100 mg of Mg-Al-O.

Reaction pathways with methyl ketones

The temporal progression of the reaction over Mg-Al-O was monitored to determine the relative reactivity of 2-hexanone and dimer/cyclic trimer condensates (**2**/**3**) (Scheme 2). Figure 4 shows a plot of the products observed as a function of time. Over half

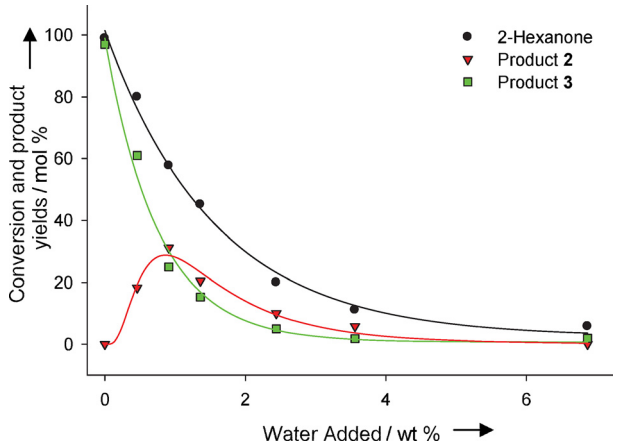

Figure 3. Effect of water addition on the activity of Mg-Al-O. Conditions: 2-hexanone (2 mmol), toluene (3 mL), water (as shown), 150 °C, 3 h, 200 mg of Mg-Al-O.

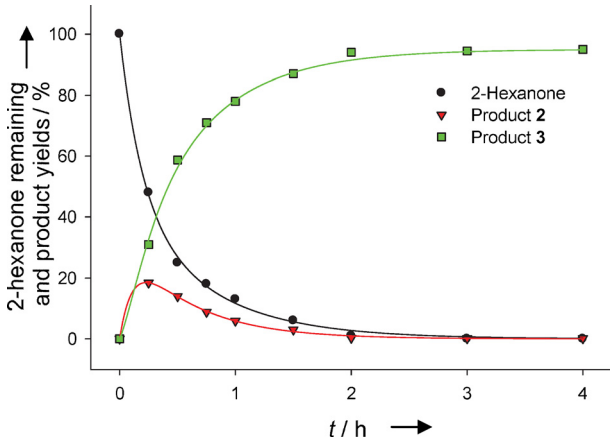

Figure 4. Product evolution during the self-condensation of 2-hexanone. Conditions: 2-hexanone (2 mmol), toluene (3 mL), 150 °C, 200 mg of Mg-Al-O.

of the initial 2-hexanone was converted to a mixture of **2** and **3** within 15 min. The dimer condensate (**2**) was then rapidly converted into the cyclic trimer condensate (**3**). A 94% yield to cyclic trimer condensates (**3**) then formed within 2 h and did not undergo further reaction. The relative reactivity of **2** over Mg-Al-O shown in Figure 4 is in stark contrast to what was observed over hydroxyapatite and strontium titanate (Table 1, entries 13 and 17), in which cases dimer condensates accumulated in yields of 46% and 55%, respectively.

An overall reaction network showing plausible intermediates and products formed during acid/base-catalyzed self-condensation of alkyl methyl ketones is presented in Scheme 2. These products are formed via either enolates or enols of the reactant ketone depending on the nature of the catalyst employed (base or acid, respectively). Dimer condensates **2a** and **2b** are formed through 1,2-addition of enolate or enol intermediates to a ketone. Cyclic trimer condensates **3a–d** could originate from 1,2- and/or 1,4-addition (Michael addition) of enolate intermediates of **1** and dimers **2a** and **2b** (Scheme 2) under basic conditions. Under acidic conditions, the aromatic condensates **5a** and **5b** are obtained exclusively from the acyclic trimer isomers of **4** via acid-promoted trienol formation followed by 6π-cyclization (Scheme 2). Reaction mechanisms for the formation of dimer and trimer condensates shown in Scheme 2 can be found in the Supporting Information. Formation of higher oligomer condensates from **3** is largely prevented by the significant steric hindrance around the reactive centers of the molecule.

The isomer distributions for condensates derived from the self-condensation of 2-butanone through 2-heptanone are given in Table 3. Although there are several possible intermediates (**I–IV**) for formation of **3a–d**, the formation of intermediate **I** by 1,4-addition (Michael addition) is preferred in the presence of a base catalyst. This preference is reflected in the isomer distribution of trimer condensates of 2-hexanone (Table 3, entry 3). The increased selectivity to **3a** (84%) from 2-hexanone also indicates that the reaction proceeds predominantly by kinetic enolate intermediates (Scheme 2).

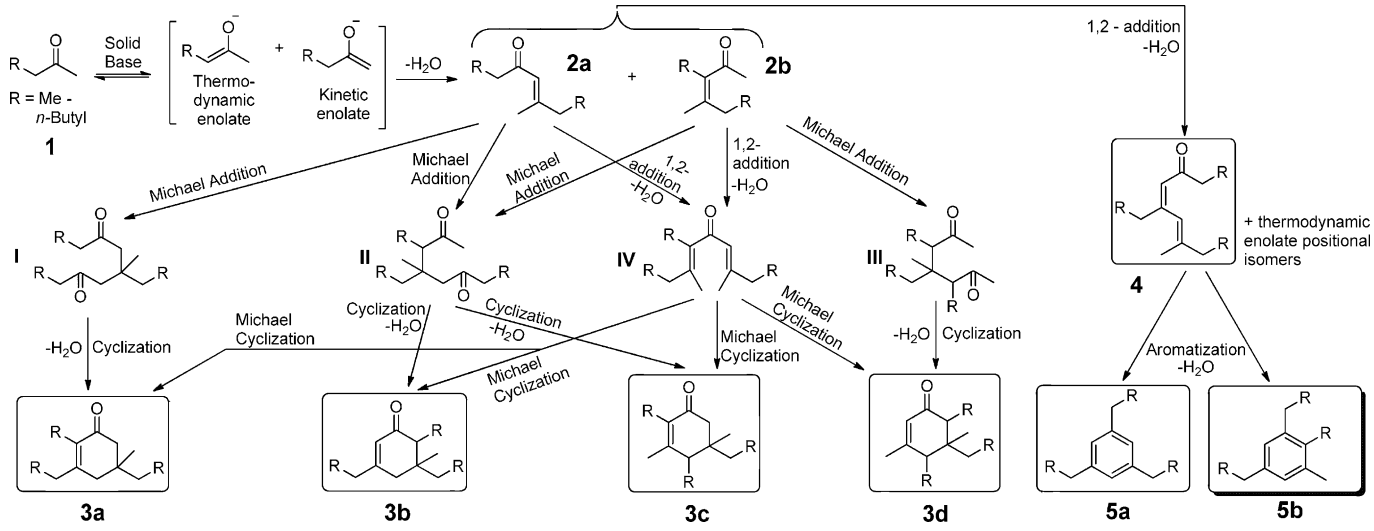

Scheme 2. Overview of plausible pathways to trimer condensates from methyl ketones.

Table 3. Specific activity and product yield from condensation of C_4–C_7 alkyl methyl ketones.[a]

Entry	Methyl ketone (**1**)	Conv. of **1** [%]	Dimers (**2**) [%]	Cyclic trimers (**3**) [%] (**3a**)	(**3b**)	(**3c**)	(**3d**)	total	Acyclic trimers (**4**) [%]	Higher oligomers [%]
1	2-butanone	98	0	53	33	6	0	92	2	5
2	2-pentanone	99	1	82	14	0	0	96	2	1
3	2-hexanone	99	1	84	11	0	0	95	2	1
4	2-heptanone	95	2	80	10	0	0	90	2	1

[a] Reagents and conditions: Methyl ketone (2 mmol), toluene (3 mL), 170 °C, 2 h, 100 mg of Mg-Al-O.

While the reactivity of the shown methyl ketones are nearly equal, as evidenced by similarly high conversions (95–99%), the distribution of condensates formed from 2-butanone (Table 3, entry 1) was different from the rest of the starting materials in Table 3. Notably, the distribution of cyclic trimer condensates **3a**–**d** indicates a significant increase in reactivity of the thermodynamic enolate formed from 2-butanone compared to that formed from 2-hexanone via intermediate **II** and/or **IV**. This difference in reactivity is due to the steric hindrance associated with the respective alkyl substituents. For all the biomass-derived methyl ketones investigated, 2-butanone is the only reactant for which isomer **3c** (Scheme 2) was observed in any significant concentration (6%). Also, the high reactivity of 2-butanone enolates together with lesser steric hindrance around the reactive centers of cyclic trimer condensates formed from 2-butanone leads to increased formation of higher oligomer condensates (5%, entry 1). For 2-pentanone through 2-heptanone (Table 3, entries 2–4), the distribution remains consistent, implying that, over this range, the length of the *n*-alkyl group has a limited effect on the reactivity of the starting ketone.

The rate of condensation is greatly diminished, however, when the alkyl group is branched, especially when the branching is proximate to the reactive centers of the ketone. In this case, the selectivity shifts significantly to dimers. For example, ketones such as 3,3-dimethylbutan-2-one and 4,4-dimethylpentan-2-one form dimers in yields of 64% and 81%, respectively, after 16 h of reaction (see Supporting Information). Decreased steric hindrance in 3-methylbutan-2-one and 4-methylpentan-2-one leads to slightly higher conversion compared to their more hindered counterparts (89% and 99% vs. 68% and 87%, respectively) and notably increased formation of **4**, **5**, and higher oligomers. Reactions with internal ketones, such as 3-pentanone and 4-heptanone also largely form dimers in yields of 44% and 9%, respectively, after 16 h. Conversely, the self-condensation of acetone is rapid, producing 39% of **3** and 57% higher oligomers after only 2 h of reaction. These results demonstrate that steric hindrance plays a profound role on both reactivity and product selectivity. It is also obvious that the exclusive formation of dimer condensates (**2**) is very difficult for *n*-alkyl methyl ketones under the optimized conditions.

The condensation of *n*-alkyl methyl ketones can be stopped at the dimer stage (**2**) if the dimer condensates can be prevented from undergoing 1,4-conjugate addition with ketone enolates. This can be achieved by in situ hydrogenation of the olefinic functionality of **2** immediately after its formation. The hydrogen required for this process can also be generated in situ from an alcohol by transfer hydrogenation in the presence of Pd.[18]

In the selective dimerization approach, 2-hexanol served as a suitable source for the in situ formation of 2-hexanone and hydrogen required for the reaction. We found that the condensation predominantly produced dimer condensates as a mixture of ketones and alcohols in the presence of Pd supported on Mg-Al-O (77% combined, Scheme 3).

Cross-condensation of methyl ketones

As noted earlier, the results presented in Table 3 indicate that the rates of condensation of biomass-derived C_4–C_7 *n*-alkyl methyl ketones are similar, as are the product distributions. The next question is whether the rates of cross-condensation of these ketones are close to those of the rates of self-condensation. To this end, mixtures of ketones were subjected to reaction under conditions similar to those used for the self-condensation studies reported in Table 3. Complete consumption of all of reactants was observed after 4 h of reaction and the

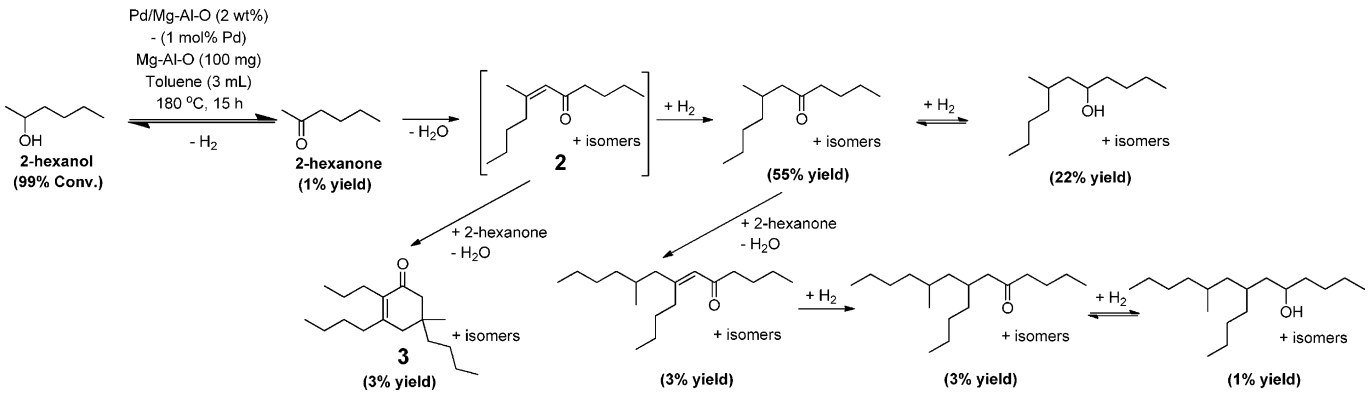

Scheme 3. Pathway for dimerization of 2-hexanol over a Pd/Mg-Al-O catalyst.

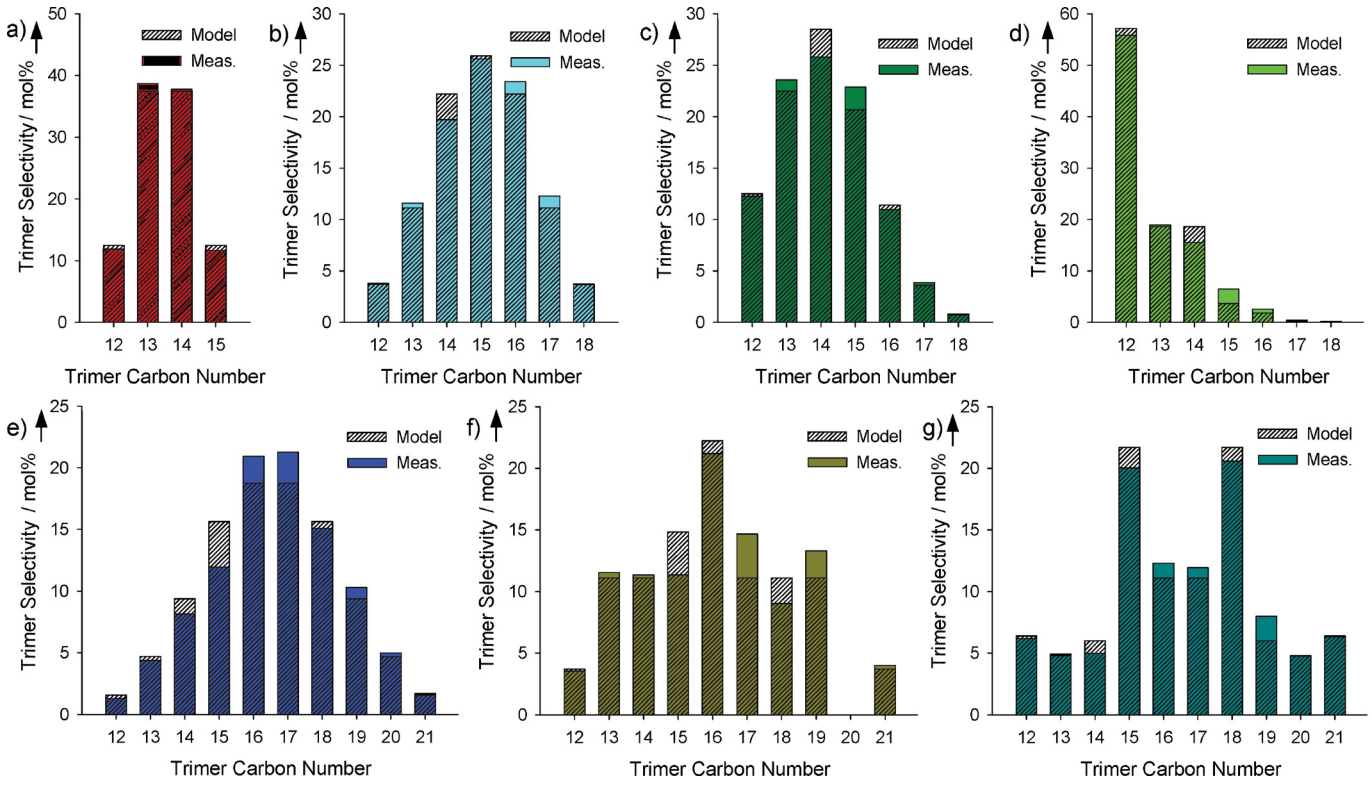

Figure 5. Product distribution of cross-condensations of mixed ketones. Conditions: methyl ketones (2 mmol), toluene (3 mL), 170 °C, 4 h, 100 mg of Mg-Al-O. a) $x_4 = 0.5$, $x_5 = 0.5$, b) $x_4 = 0.33$, $x_5 = 0.33$, $x_6 = 0.33$, c) $x_4 = 0.5$, $x_5 = 0.3$, $x_6 = 0.2$, d) $x_4 = 0.83$, $x_5 = 0.09$, $x_6 = 0.08$, e) $x_4 = 0.25$, $x_5 = 0.25$, $x_6 = 0.25$, $x_7 = 0.25$, f) $x_4 = 0.33$, $x_5 = 0.33$, $x_7 = 0.33$, g) $x_4 = 0.4$, $x_5 = 0.1$, $x_6 = 0.1$, $x_7 = 0.4$.

solid bars appearing in Figure 5 show the resulting carbon number distributions. In all of the cases shown in Figure 5, the conversion of the initial methyl ketones exceeded 99% and all observed products were trimer condensates, with the exception of trace amounts of dimers and larger oligomers. It is evident from this Figure that products containing 12 to 21 carbon atoms can be produced by the combined processes of self- and cross-condensation of C_4–C_7 methyl ketones.

If the reactivity of each methyl ketone is identical, their combination into trimers should be governed by a statistical distribution. The equation representing the trimer product distribution for a four component mixture containing 2-butanone through 2-heptanone is given by the following expression:

$$\text{Probability} = 1 = \sum_{k=4}^{7}\sum_{j=4}^{7}\sum_{i=4}^{7} x_i x_j x_k \qquad (1)$$

Here x_i, x_j, and x_k are the initial moles of alkyl methyl ketone with *i*, *j*, and *k* carbons, respectively, divided by the total initial moles of methyl ketones present, and the sum of *i*, *j*, and *k* is equal to the number of carbons in the cyclic trimer condensate formed. The sum of terms in the expanded form of Equation (1) having an identical value of $i+j+k$ (irrespective of the ordering of *i*, *j*, and *k*) may be grouped together and represent the probability of obtaining a trimer product with a given total number of carbon atoms. The shaded bars in Figure 5 give the predicted carbon number distribution based on Equation (1) for a wide range of mixtures of 2-butanone through 2-heptanone. As can be seen, the predicted and observed carbon number distributions are in close agreement, demonstrating that rates of self- and cross-condensation of each of these four methyl ketones are similar. This result also demonstrates that many component mixtures, similar to those of true fuels, may be generated with these reactions.

Hydrodeoxygenation of trimerization products

The major products produced by the self- and cross-condensation of C_4–C_7 methyl ketones (**3**) contain a cyclohexenone core. To be suitable for jet fuel, the olefin functionality and the O atom must be removed from the core structure by hydrodeoxygenation. The catalyst chosen for this step was Pt/$NbOPO_4$, based on a previous report indicating the effectiveness of this catalyst for the hydrodeoxygenation of biomass-derived compounds.[28] Accordingly, trimer condensates produced from 2-butanone and 2-hexanone were hydrogenated over Pt/$NbOPO_4$ at 160 °C in the presence of 2.8 MPa of H_2 for 5 h. Using these conditions, cyclic alkanes (**6**) were produced in quantitative yields and no evidence was found by GC–MS or high resolution mass spectrometry (HRMS) for cracking products (see Supporting Information). Based on these findings, Pt/$NbOPO_4$ was used for all further hydrodeoxygenation.

The pathways by which hydrodeoxygenation is expected to occur are illustrated in Scheme 4. The enone functionality is hydrogenated over platinum to produce the corresponding cyclohexanol derivative which then undergoes dehydration over

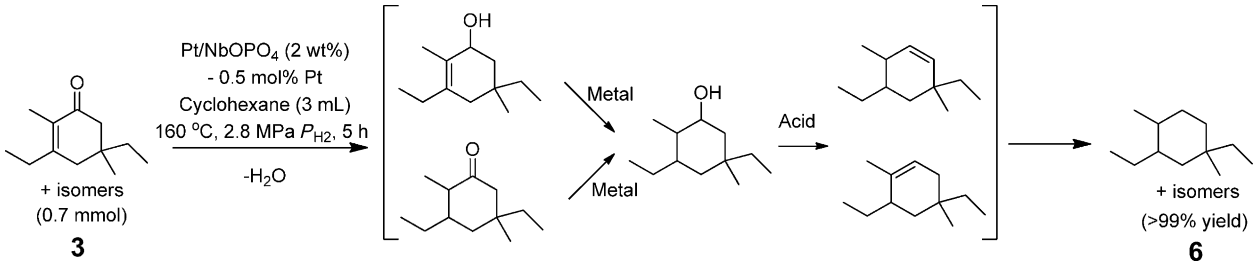

Scheme 4. Plausible reaction pathways during hydrodeoxygenation of 2-butanone trimer condensate.

acid sites on $NbOPO_4$. The intermediate alkene is then hydrogenated over platinum to form the product alkane. The optimized hydrodeoxygenation conditions were effective for various mixtures of condensates shown in Figure 5 and produced the corresponding cyclic alkanes in quantitative yields.

Properties of hydrodeoxygenated jet fuel products

The fuel properties of cyclic alkanes produced by the sequential condensation/hydrodeoxygenation of alkyl methyl ketones were evaluated and compared to those of conventional jet fuel. The mixture of C_{12} alkanes produced from 2-butanone (Table 3, entry 1) remained a clear, free-flowing liquid at $-80\,^{\circ}C$, indicating that the cloud point and pour point of this material are $< -80\,^{\circ}C$. The evaluated freezing point of the mixture was determined by ASTM D7153[29] to be $< -100\,^{\circ}C$, which far exceeds the requirements for standard Jet A and Jet A-1 blends, $-40\,^{\circ}C$ and $-47\,^{\circ}C$, respectively.[30] The kinematic viscosity of the C_{12} alkane mixture at $-20\,^{\circ}C$ was measured to be 5.5 cSt, which is significantly lower than the upper limit (8.0 cSt) specified for synthetic aviation fuel in ASTM D7566.[30b] The heat of combustion of the mixture was measured as 38.3 $MJ\,L^{-1}$ (47.0 $MJ\,kg^{-1}$), providing a volumetric energy density that is 6.1% higher than commercial Jet A fuel (36.1 $MJ\,L^{-1}$).[10]

While mixtures of C_{12} alkanes from 2-butanone condensation/hydrodeoxygenation meet or greatly exceed most fuel specifications, the inherently limited number of components in the mixture derived from entry 1 of Table 3 cannot replicate the boiling curve of jet fuel shown in Figure 6a. ASTM D7566 specifies that biomass-derived jet fuel should have at least a 15 °C increase between the 10th and 50th percentile of the boiling curve and a 40 °C difference between the 10th and 90th percentile. Furthermore, the 10th percentile must be below 205 °C and the final boiling point must be below 300 °C.[30b] To meet the boiling point distribution required for jet fuel, we also tested the properties of alkane mixtures arising from cross-condensations of a mixture of ketones as depicted in Figure 5b (C_{12}–C_{18}) and 5e (C_{12}–C_{21}). These mixtures also had low freezing points ($< -100\,^{\circ}C$) and high energy density (38.3 and 38.8 $MJ\,L^{-1}$, respectively); however, their boiling distributions still did not meet aviation fuels standards (Figure 6). In fact, the C_{12}–C_{21} mixture more closely matched the boiling curve of commercial diesel (Figure 6b),[31] and, due to its high measured derived cetane number (48.6), may be more suitable as diesel fuel.

To match the boiling distribution of jet fuel, we developed a method for identifying the optimal mixture of C_4–C_7 ketones that should be used for methyl ketone condensation/hydrodeoxygenation to form cyclic alkanes. Details of this procedure are presented in the Experimental Section and Supporting In-

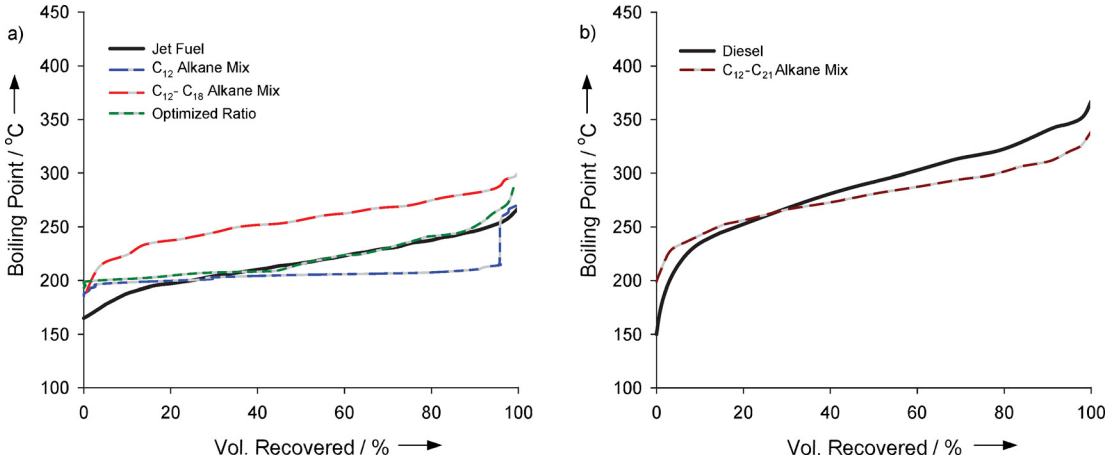

Figure 6. Simulated distillation of example mixtures. a) Distillation curves of jet fuel, hydrodeoxygenated components from Table 3, entry 1, and hydrodeoxygenated components from Figure 5b and 5d. b) Distillation curves of C_{12}–C_{21} alkanes produced from the product mixture in Figure 5e along with standard diesel fuel.

formation. Utilization of this approach indicates that the optimal fit to the boiling point distribution of conventional jet fuel can be achieved by condensation of a mixture of C_4–C_6 ketones for which $x_4 = 0.83$, $x_5 = 0.09$, $x_6 = 0.08$. The resulting distribution of C_{12}–C_{18} products is shown in Figure 5d. The simulated distillation curve for the mixture of cyclic alkanes derived from the optimized product mixture is illustrated in Figure 6a and compared with that of commercial jet fuel.[32] While this optimized mixture does meet the specifications for boiling distributions in ASTM D7566 mentioned previously, an even better fit to traditional boiling distributions of jet fuel could be made by incorporating small amounts of C_8–C_{14} alkanes produced by dimerization of C_4–C_7 ketones via the strategy shown in Scheme 3. In this way, more components with boiling points $< 200\,^{\circ}C$ could be introduced to create an ideal, biomass-derived jet fuel replacement.

Conclusions

Our work demonstrates the utility of base-catalyzed methyl ketone condensation for the selective production of condensates which, after hydrodeoxygenation, meet many specifications for jet fuel. Once methyl ketones are formed from biomass, which may occur via a broad number of pathways, yields to fuels are essentially quantitative since the small quantities of dimers and higher oligomeric products are also hydrodeoxygenated and can be blended into jet fuel at low concentrations. The optimal catalyst for condensation was found to be calcined hydrotalcite, Mg-Al-O. While this catalyst can be deactivated by water, a byproduct of methyl ketone condensation, this effect can be minimized by in situ removal of water. It was observed that if the alkyl group was highly branched, particularly at the α- or β-carbon, that the formation of dimers, rather than trimers, was favored. However, linear C_4–C_7 *n*-alkyl methyl ketones uniformly underwent condensation reactions at similar rates to form cyclic trimer condensates, which could then be converted quantitatively to substituted cyclohexane derivatives by hydrodeoxygenation over $Pt/NbOPO_4$.

Models were developed for predicting both the carbon number distribution of products formed by mixed condensation of biomass-derived C_4–C_7 *n*-alkyl methyl ketones and the boiling point distribution of the cyclic alkanes produced by hydrodeoxygenation of those products. Using these models it was possible to predict the mixture of C_4–C_6 *n*-alkyl methyl ketones required to produce the C_{12}–C_{18} cyclic alkanes which exhibit a boiling point distribution curve very close to that of conventional jet fuel. The cyclic alkanes derived from the sequence of condensation and hydrodeoxygenation possess exceptional properties with regards to freezing point and energy density. The measured freezing points are well below those specified for conventional jet fuel, and the volumetric energy density is 6% higher than that of conventional jet fuel. Our work has also shown that dimerization of secondary alcohols through bifunctional metal/base-catalyzed condensation could also provide an effective method for including condensates of 2-hexanone and 2-heptanone into the fuel supply.

Experimental Section

Materials

All purchased chemicals were used as received without further purification. Starting materials, including 2-butanone (≥99%), 2-pentanone (≥98%), 2-hexanol (99%) 2-hexanone (98%), and 2-heptanone (99%), were acquired from Sigma–Aldrich, USA.

Base catalysts, including pyridine (>99%), KF/Al_2O_3, NaOH, KOH, K_3PO_4, synthetic HAP, and hydrotalcite were purchased from Sigma–Aldrich, USA. Mg-Al-O was prepared from commercially available synthetic hydrotalcite (Sigma Aldrich) by calcination in static air at 700 °C for 2 h after a $2\,^{\circ}C\,min^{-1}$ temperature ramp. Acid catalysts, including acetic acid (≥99%) and SiO_2–Al_2O_3 (catalyst support, grade 135, 6.5% Al content) were also purchased from Sigma–Aldrich, USA. SiO_2–Al_2O_3 was activated by drying overnight at 120 °C. Niobic acid and $NbOPO_4$ were received in kind from CBMM, Brazil and were calcined in air prior to use at 300 °C for 2 h after a $2\,^{\circ}C\,min^{-1}$ temperature ramp to yield Nb_2O_5 and $NbOPO_4$. La_2O_3, MgO, Mg-Zr-O, TiO_2, ZrO_2, Ti-Zr-O, and $SrTiO_3$ were produced by solution phase precipitation and calcination. Specific synthesis procedures for each can be found in the Supporting Information along with characterization of all catalyst materials by BET and XRD.

Supported 2 wt% $Pt/NbOPO_4$ was synthesized by incipient wetness impregnation using H_2PtCl_6 hexahydrate from Sigma–Aldrich, USA. Approximately 265 mg of H_2PtCl_6 hexahydrate was dissolved in water and slowly added to 5.0 g of calcined $NbOPO_4$ while mixing and grinding in a mortar and pestle. The mixture was then heated at $2\,^{\circ}C\,min^{-1}$ to 300 °C and reduced in a constant flow of $50\,mL\,min^{-1}$ of 9% H_2 in He. Similarly, 2 wt% Pd/Mg-Al-O was synthesized by incipient wetness impregnation of $Pd(NO_3)_2$ dihydrate into Mg-Al-O. The catalyst was then calcined in air by ramping at $1\,^{\circ}C\,min^{-1}$ to 550 °C and holding at that temperature for 4 h.

Product characterization

Reactant conversion and product yield were determined for reaction mixtures by gas chromatography. After diluting reaction mixtures in dichloromethane so that desired products were in a concentration of 0.01–1.0 $mg\,mL^{-1}$, the mixtures were analyzed with a Varian CP-3800 gas chromatograph equipped with a flame ionization detector (FID) and Varian 320-triple quadrupole mass spectrometer. Good separation of products was obtained using a Factor-Four VF-5 capillary column. Individual product peaks were identified by mass spectrometry and structures were confirmed with NMR and FTIR spectroscopy of selected purified compounds (Supporting Information). Quantification was achieved by adding a known quantity of dodecane or nonane as an internal standard. Calibration curves were generated for all reactants and the purified products of reaction of 2-butanone and 2-hexanone. Response factors for other condensation products were calculated using the effective carbon number method, which has been shown to predict FID response factors within 1.7%.[33] For the purposes of this paper, yield and selectivity are defined by Equations (2) and (3):

$$\text{Yield} = \frac{n_{\text{Product}}}{n_{\text{Reactant,initial}}} \times \text{Stoichiometric Factor} \times 100\,\% \quad (2)$$

$$\text{Selectivity} = \frac{n_{\text{Product}}}{n_{\text{Reactant,initial}} - n_{\text{Reactant}}} \times \text{Stoichiometric Factor} \times 100\,\% \quad (3)$$

in which $n_{Product}$ = mol of product at a given time; $n_{Reactant}$ = mol of reactant at a given time; $n_{Reactant,initial}$ = mol of reactant fed; stoichiometric factor = stoichiometric number of reactant mol per mol of product.

Catalyst characterization

The surface area of each catalyst was measured prior to use by Brunauer–Emmett–Teller (BET) analysis. After degassing at 180 °C for 6 h in a stream of flowing Ar, samples were placed onto a Micromeritics TriStar unit and the BET isotherms were measured. X-ray powder patterns were measured by X-ray diffraction to determine the crystallographic phases of catalyst materials over a 2θ range of 10–80 degrees or 20–60 degrees, with a step size of 0.02 degrees on a Bruker D8 instrument. Metal dispersion was assessed by CO pulse chemisorption using a Micromeritics AutoChem II chemisorption analyzer. Metal nanoparticles were reduced by a mixture of 10% H_2 in Ar at 250 °C for 30 min prior to CO adsorption. The cumulative quantity of CO adsorbed was then used to determine metal dispersion and particle size for Pt/$NbOPO_4$ and Pd/Mg-Al-O (Supporting Information).

Base-catalyzed condensation reactions

In a typical experiment, 2 mmol of methyl ketone substrate, 144 mg of dodecane (internal standard), and 3 mL of toluene was added to a 12 mL glass Q-tube reactor purchased from QLabtech. A polytetrafluoroethylene (PTFE)-coated stirbar and 50–200 mg of Mg-Al-O was then added to the reactor and the reactor was sealed with a PTFE-coated silicone septum. The reactor was then immersed in a preheated oil bath at 150–170 °C and stirred magnetically at 500 rpm for the duration of reaction. Upon completion of the reaction, the Q-tube reactor was removed and cooled. Approximately 1.5 mL of product mixture was then removed and centrifuged at 14000 rpm to separate the catalyst. The supernatant was then diluted with dichloromethane and products were analyzed by GC.

Metal/base-catalyzed reactions to dimer condensates

Approximately 2 mmol of 2-hexanol, 144 mg of dodecane (internal standard), and 3 mL of toluene was added to a 12 mL glass Q-tube reactor. The Pd/Mg-Al-O (2 wt% Pd) catalyst was then added to the reactor at a loading of 1 mol% of Pd (with respect to 2-hexanol). Under optimized conditions, an additional 100 mg of Mg-Al-O was further added to increase the basic loading. A PTFE-coated stir-bar was then added to the reactor and the reactor was sealed with a PTFE-coated silicone septum. The reactor was then immersed in a preheated oil bath at 180 °C and stirred magnetically at 500 rpm for 15 h. Upon completion of the reaction, the Q-tube reactor was removed from the oil bath and processed in the same manner as base-catalyzed condensation reactions.

Hydrodeoxygenation reactions

Hydrodeoxygenation reactions were carried out in an eight-unit HEL ChemSCAN autoclave system. In a typical experiment, 0.67 mmol of cyclic trimer condensates, 144 mg of nonane (internal standard), 3 mL of cyclohexane, and 0.25–0.5 mol% Pt/$NbOPO_4$ (total metal content basis) was added to the HEL Hastelloy autoclave reactor. A PTFE-coated stirbar was attached to the reactor system and the autoclave was sealed. The reactor was purged three times with N_2 and H_2 prior to heating to reaction temperature. After stirring the reaction at 500 rpm for 5 h, the reactors were cooled to room temperature and opened. Approximately 1.5 mL of product mixture was then removed and centrifuged at 14000 rpm to separate the catalyst. The supernatant was then diluted with dichloromethane and products were analyzed by GC.

Measurement of boiling curves by simulated distillation

Simulated distillation was used to evaluate the suitability of alkane product distributions for replacement of traditional jet fuel blends using small quantities of synthesized materials. GC retention times for known C_7–C_{20} *n*-alkanes measured during linearly temperature-ramped gas chromatography were correlated with the boiling points of these compounds (Supporting Information).[34] Using this correlation, any alkane mixture containing components with boiling points within this boiling range could be analyzed to determine the boiling curve of the mixture. Individual product peaks were integrated and their boiling points were determined by their elution time. The boiling distribution curve was then generated by the cumulative sum of the individual components. For the purposes of this work, we have assumed that the alkane components derived from mixed condensations may be approximated to be of uniform density. This assumption makes it possible to compare the gravimetric recovery data provided by simulated distillation and the volumetric recovery distillation curves of standard jet fuels. The validity of the assumption was established by measuring the bulk density of the alkane blends shown in Figure 6. These measured densities varied by less than 0.5% from the mean despite differences in the composition of the compounds.

Modeling the boiling curve of methyl ketone mixtures

The following procedure was used to identify the mixture of C_4–C_7 *n*-alkyl methyl ketones needed to produce (via ketone condensation and subsequent hydrodeoxygenation of the resulting product) a mixture of alkyl substituted cyclohexane derivatives with a specified boiling point distribution. The alkane boiling regions associated with each of the cyclic products were identified by GC–MS (Supporting Information). We then approximated the collection of individual components in each carbon number range by a Gaussian probability distribution (standard deviation and means provided in Supporting Information). The area under each Gaussian curve was normalized to the mass percent of that product predicted by Equation (1). In this way, the quantity of products in each carbon number range was predicted by Equation (1), and the boiling curve of those products was determined by their respective Gaussian distributions.

The cumulative integration of all Gaussian curves was then used to predict the boiling distribution curve of mixtures. Using this strategy, a system of equations was generated to predict the boiling distribution of any set of products produced from any initial mixture of 2-butanone, 2-pentanone, and 2-hexanone. Because x_4, x_5, and x_6 must sum to 1 for this three methyl ketone mixture, only two independent variables (x_4 and x_5) were required to generate any possible boiling curve for hydrodeoxygenated cyclic trimers of these materials. The exceptional agreement between this predictive boiling model and the measured simulated distillation curve can be seen in the Supporting Information. The method described above was used to determine the optimal mixture of ketones required to produce a product that minimizes the squared residuals between the commercial jet fuel and the predicted boiling curve. A contour plot showing regions of minimal differences between

jet fuel and the produced mixture of alkanes can be found in the Supporting Information.

Acknowledgements

This work was supported by the Energy Biosciences Institute. E.R S. also acknowledges support from a National Science Foundation Graduate Research Fellowship under Grant No. DGE 1106400. The authors would also like to acknowledge the contributions of Alice Yeh towards Dean–Stark experiments in the Supporting Information.

Keywords: biofuels · C–C coupling reactions · heterogeneous catalysis · hydrogenation · jet fuel

[1] J. Han, A. Elgowainy, H. Cai, M. Q. Wang, *Bioresour. Technol.* **2013**, *150*, 447.
[2] a) M.-O. P. Fortier, G. W. Roberts, S. M. Stagg-Williams, B. S. M. Sturm, *Appl. Energy.* **2014**, *122*, 73; b) P. Gegg, L. Budd, S. Ison, *J. Air Transp. Manage.* **2014**, *39*, 34.
[3] A. Milbrandt, C. Kinchin, R. McCormick, The Feasibility of Producing and Using Biomass-Based Diesel and Jet Fuel in the United States, (NREL) NREL/TP-6A20-58015, **2013**.
[4] a) C. Somerville, H. Youngs, C. Taylor, S. C. Davis, S. P. Long, *Science* **2010**, *329*, 790; b) J. Janaun, N. Ellis, *Renewable Sustainable Energy Rev.* **2010**, *14*, 1312; c) G. W. Huber, S. Iborra, A. Corma, *Chem. Rev.* **2006**, *106*, 4044.
[5] T. Kalnes, T. Marker, D. R. Shonnard, *Int. J. Chem. React. Eng.* **2007**, *5*, A48.
[6] M. Balakrishnan, E. R. Sacia, A. T. Bell, *ChemSusChem* **2014**, *7*, 1078.
[7] a) A. Corma, O. de La Torre, M. Renz, N. Villandier, *Angew. Chem. Int. Ed.* **2011**, *50*, 2375; *Angew. Chem.* **2011**, *123*, 2423; b) A. Corma, O. de La Torre, M. Renz, *Energy Environ. Sci.* **2012**, *5*, 6328; c) G. Li, N. Li, J. Yang, L. Li, A. Wang, X. Wang, Y. Cong, T. Zhang, *Green Chem.* **2014**, *16*, 594.
[8] J. Q. Bond, D. M. Alonso, D. Wang, R. M. West, J. A. Dumesic, *Science* **2010**, *327*, 1110.
[9] M. Mascal, S. Dutta, I. Gandarias, *Angew. Chem. Int. Ed.* **2014**, *53*, 1854; *Angew. Chem.* **2014**, *126*, 1885.
[10] E. G. Eddings, S. H. Yan, W. Ciro, A. F. Sarofim, *Combust. Sci. Technol.* **2005**, *177*, 715.
[11] B. G. Harvey, M. E. Wright, R. L. Quintana, *Energy Fuels* **2010**, *24*, 267.
[12] J. Yang, N. Li, G. Li, W. Wang, A. Wang, X. Wang, Y. Cong, T. Zhang, *Chem. Commun.* **2014**, *50*, 2572.
[13] X.-J. Ji, H. Huang, P.-K. Ouyang, *Biotechnol. Adv.* **2011**, *29*, 351.
[14] a) A. Multer, N. McGraw, K. Hohn, P. Vadlani, *Ind. Eng. Chem. Res.* **2013**, *52*, 56; b) A. V. Tran, R. P. Chambers, *Biotechnol. Bioeng.* **1987**, *29*, 343; c) R. R. Emerson, M. C. Flickinger, G. T. Tsao, *Ind. Eng. Chem. Prod. RD* **1982**, *21*, 473.
[15] Y. Gong, L. Lin, J. B. Shi, S. J. Liu, *Molecules* **2010**, *15*, 7946.
[16] K. Min, S. Kim, T. Yum, Y. Kim, B.-I. Sang, Y. Um, *Appl. Microbiol. Biotechnol.* **2013**, *97*, 5627.
[17] T. Thananatthanachon, T. B. Rauchfuss, *Angew. Chem. Int. Ed.* **2010**, *49*, 6616; *Angew. Chem.* **2010**, *122*, 6766.
[18] P. Anbarasan, Z. C. Baer, S. Sreekumar, E. Gross, J. B. Binder, H. W. Blanch, D. S. Clark, F. D. Toste, *Nature* **2012**, *491*, 235.
[19] G. W. Huber, J. N. Chheda, C. J. Barrett, J. A. Dumesic, *Science* **2005**, *308*, 1446.
[20] a) J. I. Di Cosimo, V. K. Díez, C. R. Apesteguía, *Appl. Catal. A* **1996**, *137*, 149; b) J. I. Di Cosimo, C. R. Apesteguía, *J. Mol. Catal. A* **1998**, *130*, 177; c) V. A. Bell, H. S. Gold, *J. Catal.* **1983**, *79*, 286; d) C. P. Kelkar, A. A. Schutz, *Appl. Clay Sci.* **1998**, *13*, 417; e) R. M. West, E. L. Kunkes, D. A. Simonetti, J. A. Dumesic, *Catal. Today* **2009**, *147*, 115.
[21] H. J. Seebald, W. Schunack, *Arch. Pharm.* **1972**, *305*, 785.
[22] J. R. Walton, B. Yeomans, (USPTO), US3981918A, **1976**.
[23] W. B. Renfrow, A. Renfrow, *J. Am. Chem. Soc.* **1946**, *68*, 1801.
[24] J. T. Kozlowski, R. J. Davis, *ACS Catal.* **2013**, *3*, 1588.
[25] a) A. Corma, V. Fornés, R. M. Martín-Aranda, F. Rey, *J. Catal.* **1992**, *134*, 58; b) A. Corma, V. Fornes, F. Rey, *J. Catal.* **1994**, *148*, 205; c) M. J. Climent, A. Corma, S. Iborra, K. Epping, A. Velty, *J. Catal.* **2004**, *225*, 316; d) A. Corma, S. B. A. Hamid, S. Iborra, A. Velty, *J. Catal.* **2005**, *234*, 340.
[26] Y. Liu, E. Lotero, J. G. Goodwin, X. Mo, *Appl. Catal. A* **2007**, *331*, 138.
[27] a) S. K. Sharma, P. A. Parikh, R. V. Jasra, *J. Mol. Catal. A* **2007**, *278*, 135; b) E. R. Sacia, M. H. Deaner, Y. L. Louie, A. T. Bell, *Green Chem.* **2015**, *17*, 2393.
[28] a) R. M. West, M. H. Tucker, D. J. Braden, J. A. Dumesic, *Catal. Commun.* **2009**, *10*, 1743; b) N. Li, G. A. Tompsett, G. W. Huber, *ChemSusChem* **2010**, *3*, 1154; c) W. Xu, Q. Xia, Y. Zhang, Y. Guo, Y. Wang, G. Lu, *ChemSusChem* **2011**, *4*, 1758.
[29] ASTM D7153-05: Standard Test Method for Freezing Point of Aviation Fuels (Automatic Laser Method), ASTM International, **2010**.
[30] a) ASTM D1655-14: Standard Specification for Aviation Turbine Fuels, ASTM International, **2013**; b) ASTM D7566-14a: Standard Specification for Aviation Turbine Fuel Containing Synthesized Hydrocarbons, ASTM International, **2013**.
[31] C. Vendeuvre, R. Ruiz-Guerrero, F. Bertoncini, L. Duval, D. Thiébaut, M.-C. Hennion, *J. Chromatogr. A* **2005**, *1086*, 21.
[32] G. Hemighaus, T. Boval, J. Bacha, Fred Barnes, M. Franklin, L. Gibbs, N. Hogue, J. Jones, D. Lesnini, J. Lind, J. Morris, *Aviation Fuels Technical Review*, Chevron Global Aviation, **2006**.
[33] a) T. Holm, *J. Chromatogr. A* **1999**, *842*, 221; b) A. D. Jorgensen, K. C. Picel, V. C. Stamoudis, *Anal. Chem.* **1990**, *62*, 683; c) J. T. Scanlon, D. E. Willis, *J. Chromatogr. Sci.* **1985**, *23*, 333.
[34] ASTM D2887 – 13: Standard Test Method for Boiling Range Distribution of Petroleum Fractions by Gas Ghromatography, ASTM International, **2013**.

Received: January 1, 2015
Published online on April 17, 2015